DOI: 10.1002/anie.200802393

Clathrates

Toward Functional Clathrasils: Size- and Composition-Controlled Octadecasil Nanocrystals by Desilication**

Javier Pérez-Ramírez, Sònia Abelló, Luis A. Villaescusa, and Adriana Bonilla*

Zeolites are a unique class of crystalline aluminosilicates with very high surface areas, which are a consequence of ordered micropores and cavities of molecular dimensions (0.25–1 nm) that enable shape-selective catalytic transformations. To date, 179 different zeolite structures have been reported,[1] enabling pore engineering and offering seemingly endless possibilities to tailor these materials for chemical reactions. However, the sole presence of micropores in zeolites often imposes diffusion limitations owing to restricted access and slow transport to and from the active site,[2] thus resulting in low utilization of the zeolite active volume in catalyzed reactions. This situation represents a major drawback in most industrial reactions over zeolites (ZSM-5, mordenite, beta, ferrierite), for example, cracking, (hydro)isomerization, and alkylation, as they do not operate at their full potential. Strategies for improved accessibility and molecular transport comprise the preparation of zeolites with wide and multidirectional pores[3] or with short diffusion length. The latter can be attained by nanosized zeolites (crystals typically smaller than 200 nm),[4] delaminated zeolites,[5] zeolite composites,[6] and mesoporous zeolite crystals.[7] To pursue these structures, a number of templated and nontemplated synthetic routes have been developed in recent years.[8]

The problem of accessibility in nanoporous solids is extreme in zero-dimensional clathrasils, that is, zeolite-related materials consisting of window-connected cages. Examples of these compounds are sodalite (SOD), sigma-2 (SGT), dodecasil 1H (DOH), dodecasil 3C (MTN), nonasil (NON), and octadecasil (AST).[1] The pore openings in these caged structures are restricted to six-membered rings of $[SiO_4]$ units at most, which corresponds to pore diameters of approximately 0.2 nm.[9] These pores are too small for the removal of templates and, afterwards, are impenetrable to typical sorbate molecules such as N_2 or reactants such as hydrocarbons. Therefore, the intrinsic topology of clathrasils makes them "blinded" porous materials without current perspective for catalytic applications. Herein we report for the first time a simple approach for the fabrication of clathrasil nanocrystals. For this purpose, controlled extraction of silicon in aluminum-containing octadecasil by treatment in alkaline medium was accomplished. This demetallation method, known as desilication, has to date been applied to generate intracrystalline mesoporosity in channel-type zeolites (ZSM-5, ZSM-12, and mordenite) with framework Si/Al ratios in the optimal window of 25–50.[10] We have optimized treatment conditions (base, concentration, temperature, and time) to obtain uniform octadecasil nanocrystals (10–25 nm) with high external surface areas (up to 200 $m^2 g^{-1}$) and no deterioration of the pristine clathrasil structure. We demonstrate that the octadecasil nanocrystals catalyze the pyrolysis of polyethylene. These results bring us closer to functional clathrasils, thus clearing the way for applications in catalysis.

Octadecasil is the all-silica ($Si_{20}O_{40}$) counterpart of the AlPO-16 structure and consists of rhombododecahedral [$4^6 6^{12}$] cages, which are linked together with hexahedral [4^6] cages, commonly referred to as double four-ring (D4R) units (Figure 1, right).[11] As described in the Experimental Section, octadecasil with a nominal framework ratio Si/Al = 30 was synthesized hydrothermally in fluoride medium using

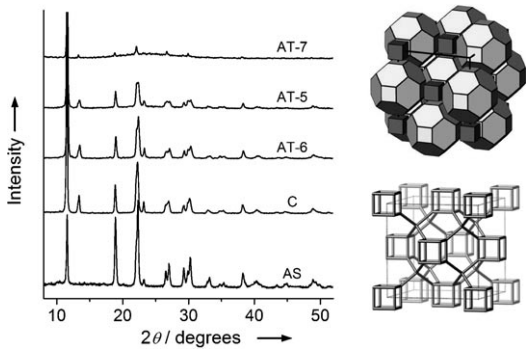

Figure 1. X-ray diffraction patterns of the as-synthesized (AS), calcined (C), and alkaline-treated (AT) octadecasil samples (left) and representation of the octadecasil structure[1] (right). Codes and treatment conditions are given in Table 1.

N,*N*,*N*-trimethyl-*tert*-butylammonium ($TMTBA^+$) as the structure-directing agent (SDA). Previous studies[11] revealed that F^- ions are located in the center of the D4Rs, whereas $TMTBA^+$ ions fill the large rhombododecahedral cages, thus attaining charge-matching in the all-silica neutral framework. Aluminum can be isomorphously substituted in the frame-

[*] Prof. Dr. J. Pérez-Ramírez, Dr. S. Abelló, Dr. A. Bonilla
Institute of Chemical Research of Catalonia (ICIQ)
Avinguda Països Catalans 16, 43007 Tarragona (Spain)
Fax: (+34) 977-920-224
E-mail: jperez@iciq.es
Prof. Dr. J. Pérez-Ramírez
Catalan Institution for Research and Advanced Studies (ICREA)
Passeig Lluís Companys 23, 08010 Barcelona (Spain)
Dr. L. A. Villaescusa
Dpto. Química, Universidad Politécnica de Valencia
Camino de Vera s/n, 46071, Valencia (Spain)

[**] This research was supported by the MEC (projects CTQ2006-01562PPQ, PTQ05-01-00980, and Consolider-Ingenio 2010, grant CSD2006-003) and the ICIQ Foundation.

Supporting information for this article is available on the WWW under http://dx.doi.org/10.1002/anie.200802393.

work in a wide range of Si/Al ratios,[12] $[SiO_2]_{20-n}[AlO_2]_n[TMTBAF_{1-n/2}]_2$, where n is the number of aluminum atoms per unit cell. Thus, tetrahedral Al^{III} competes with F^- to balance the positive charge of the SDA. The XRD pattern of the as-synthesized aluminum-containing octadecasil (AS, Figure 1) shows the characteristic reflections of the tetragonal crystal structure, confirming the high crystallinity and purity of the sample. According to the above considerations and chemical analysis, the unit cell composition is given by $[SiO_2]_{19.37}[AlO_2]_{0.63}[TMTBA]_2F_{1.37}$.

The template was completely removed, together with fluoride, by calcination of the as-prepared sample in static air at 1223 K for 5 h, as confirmed by carbon analysis and thermogravimetry (see Figure S1 in the Supporting Information). The infrared spectrum of the calcined sample (Figure 2) reveals the disappearance of CH vibrations around 3000 cm^{-1}, which are associated with the template. Calcination leads to the appearance of silanol groups at 3740, 3730, and 3550 cm^{-1}.

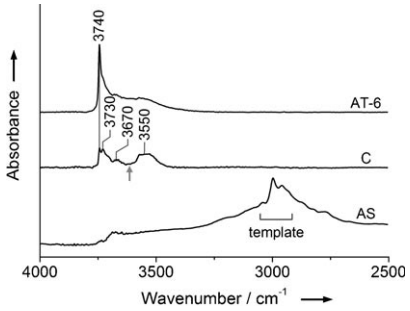

Figure 2. Infrared spectra of the as-synthesized, calcined, and alkaline-treated octadecasil samples. Traces are shifted vertically for clarity.

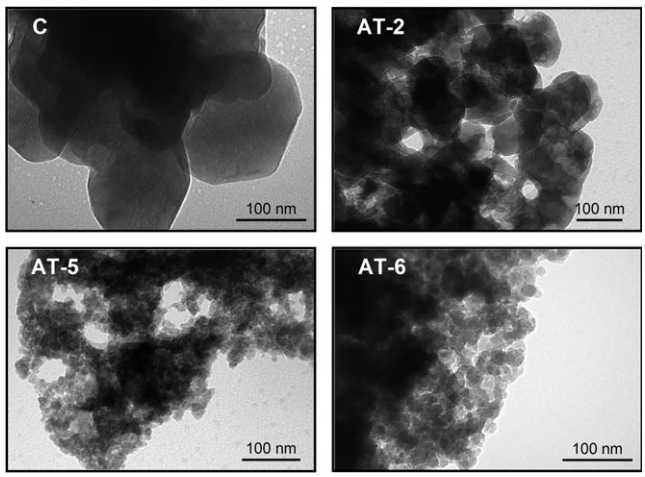

Figure 3. Transmission electron micrographs of selected octadecasil samples.

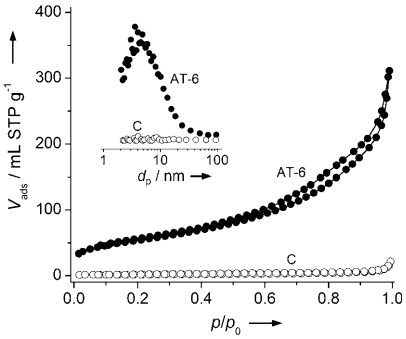

Figure 4. Nitrogen isotherms of the calcined and alkaline-treated octadecasil samples. p/p_0 = relative pressure. Inset: Barrett–Joyner–Halenda (BJH) adsorption pore size distributions. d_p = pore diameter.

No absorption band around 3610 cm^{-1}, characteristic of Brønsted acidity,[13] was observed (arrow in Figure 2). In line with ^{27}Al magic-angle spinning NMR spectroscopy studies,[11c] this result indicates the dislodgment of framework aluminum during the high-temperature thermal treatment. Related to this finding, the infrared spectrum shows a low-intensity absorption at 3670 cm^{-1}, assigned to hydroxyl groups connected to extraframework aluminum species.[13] The Si/Al ratio in the calcined sample was 31, that is, very close to the ratio of 30 in the synthesis gel. Despite the high-temperature treatment required to remove guest species from the as-synthesized sample, the structure of the clathrasil is preserved (XRD of C in Figure 1). The morphology of the calcined octadecasil determined by TEM consisted of poorly faceted 100–200 nm crystals (Figure 3). As expected, the N_2 isotherm of the sample (Figure 4) indicated essentially no uptake, owing to the inaccessibility of the cage-like voids by nitrogen. The micropore volume was zero, and the low mesopore surface area (6 m^2g^{-1}, Table 1) accounts for the external surface of the crystals.

Alkaline treatments of calcined octadecasil were conducted with varying base, concentration, temperature, and time (Table 1). The optimal treatment reported for ZSM-5 and mordenite (0.2 M NaOH, 338 K, 30 min)[10b,d] led to limited mesoporosity development in octadecasil (AT-3, $S_{meso} = 26\ m^2g^{-1}$), suggesting that harsher conditions are required for silicon leaching out of the clathrate. As expected,

Table 1: Porous properties determined by N_2 adsorption of the calcined and alkaline-treated octadecasil samples.

Sample	Agent	c [M]	T [K]	t [min]	V_{pore} [mL g^{-1}]	S_{meso}[a] [m^2g^{-1}]	Yield[b] [%]
C	–	–	–	–	0.02	6	–
AT-1	NaOH	0.2	318	30	0.05	9	86
AT-2	NaOH	0.2	338	15	0.08	13	80
AT-3	NaOH	0.2	338	30	0.11	26	70
AT-4	NaOH	0.2	338	60	0.28	94	49
AT-5	NaOH	0.2	338	90	0.31	145	49
AT-6	NaOH	0.2	358	30	0.42	191	41
AT-7	NaOH	0.2	358	90	0.37	139	51
AT-8	NaOH	1.0	338	30	0.27	35	65
AT-9	NaOH	0.05	338	30	0.05	12	88
AT-10	NH_4OH	0.2	338	30	0.03	9	90
AT-11	Na_2CO_3	0.2	338	30	0.05	19	86
AT-12	Na_2CO_3	0.2	338	300	0.05	16	88

[a] t-plot method.[14] [b] Grams of solid after workup per gram of sample treated.

NaOH treatments using more diluted solution, lower temperature, or shorter time induced minor changes in the textural properties of the material. Increasing the NaOH concentration to 1M slightly increased S_{meso}. In contrast, exposing octadecasil to the alkaline solution for longer times and at higher temperature boosted the porosity of the treated materials. For example, AT-5 (0.2M NaOH, 338 K, 90 min) and AT-6 (0.2M NaOH, 358 K, 30 min) have $S_{meso} = 145$ and 191 $m^2 g^{-1}$, respectively, that is, 30 times higher than in the parent sample. Total pore volumes around 0.4 $mL g^{-1}$ were attained. Other bases, such as NH_4OH and Na_2CO_3, were found to be less effective than NaOH (Table 1).

The effect of the alkaline treatment in the nitrogen isotherm of the clathrate is spectacular (Figure 4). The parent octadecasil sample, with no measurable porosity owing to inaccessibility, transforms into a mesoporous material displaying substantial N_2 uptake over a wide range of relative pressures (type IIb isotherm). The AT-6 sample shows a fairly uniform pore size distribution centered at 5 nm (inset Figure 4). Despite drastic porosity changes caused by NaOH treatment, the crystalline structure of octadecasil in the mesoporous AT-5 and AT-6 samples is truly preserved (Figure 1). However, alkaline treatment under more severe conditions, for example, AT-7 (0.2M, 358 K, 90 min), caused serious structural damage, as revealed by the decreased intensity of the diffraction lines as well as the appearance of a very broad reflection clearly signaling sample amorphization. These results indicate that the desilication treatment by alkaline solutions should be carefully optimized to generate substantial mesoporosity in the clathrasil without altering its pristine crystal structure.

Further insight into the mechanism of silicon extraction and the nature of the mesoporosity in the clathrasil was obtained. Attenuated total reflection infrared (ATR-IR) spectroscopy enabled us to monitor in situ the process of silicon extraction upon NaOH treatment (see Figure S2 in the Supporting Information). As reported for ZSM-5 and mordenite,[10b,d] silicon leaching in alkaline medium is favored over aluminum, that is, the treatment is highly selective toward silicon extraction. As shown in Table 2, the concentration of aluminum in the filtrates is more than two orders of magnitude lower than the concentration of silicon (in the filtrate, Si/Al > 300). Owing to the preferential silicon removal, the Si/Al ratio of 31 in sample C decreased to 13 in AT-6. An excellent correlation was obtained between the increased amount of silicon dissolved in alkaline medium, the decreased Si/Al ratio in the resulting solid, and the increase in mesopore surface area. Accordingly, as an additional attractive feature of desilication, mesoporosity development is accompanied by the progressive enrichment of the octadecasil crystals in aluminum. Upon alkaline treatment, the sample developed isolated silanol groups, and hydroxyl nests vanished. This change is evidenced in the infrared spectrum of AT-6 (Figure 2) by the increased intensity of the band at 3740 cm^{-1} and the disappearance of the broad band at 3550 cm^{-1}. The weak absorption at 3670 cm^{-1} arising from extraframework aluminum is practically unchanged in both calcined and alkaline-treated samples.

Table 2: Chemical composition of the solid and filtrates in alkaline-treated octadecasil samples. The mesopore surface area determined from N_2 adsorption is also included.

Sample	$(Si/Al)_{solid}$ [mol mol^{-1}]	$(Si/Al)_{filtrate}$ [mol mol^{-1}]	$[Si]_{filtrate}$ [mg L^{-1}]	$[Al]_{filtrate}$ [mg L^{-1}]	S_{meso} [$m^2 g^{-1}$]
C	31	–	–	–	6
AT-3	24	295	909	2.9	26
AT-5	16	300	2040	6.5	145
AT-6	13	433	3015	6.7	191

N_2 adsorption and TEM unequivocally reveal the intercrystalline nature of the mesopores in alkaline-treated octadecasil, which differs from the intracrystalline mesoporosity upon NaOH treatment of channel-type zeolites.[10] The micropore volume in all the alkaline-treated octadecasil samples was zero, meaning that the cages in the clathrasil remain inaccessible and the mesopore surface area exclusively derives from the external surface of the modified clathrate. As seen in Figure 3, the NaOH treatment leads to nanosized octadecasil crystals by progressive dissolution of silicon in the original sample. In this manner, control can be exerted on the size of the clathrate crystals and on composition (Si/Al ratio). The nanocrystals in samples AT-5 and AT-6 are in the range of 10–25 nm, that is, one order of magnitude smaller than in the calcined octadecasil. Moreover, the size distribution is fairly homogeneous. The attack of the base starts from the external surface of the zeolite crystal. In one- and three-dimensional zeolites, the base extracts silicon by perforating into the crystal, which results in intracrystalline mesoporosity. In contrast, the zero-dimensional character of clathrasils forces the alkaline to operate in a different manner, as the cages cannot be accessed. Therefore, instead of being "perforated", the crystal is "fragmented" and "peeled" by the base, thus resulting in an enhanced external surface area (intercrystalline mesoporosity). Consequently, we infer that the dimensionality of the zeolite determines the nature of the porosity induced by selective silicon extraction.

The yield of the treatment, defined as the amount of solid in grams after the alkaline workup per gram of sample treated, ranged from 40–90%, decreasing with an increasing amount of leached silicon (Table 1). Although representative, the yield might be somewhat underestimated (by ca. 10%) owing to unavoidable solid losses during filtration of the treated dispersion and the relatively small amount of sample used in desilication experiments (166 mg). In any case, valuable conclusions on the mechanism of nanocrystal formation can be drawn. A shrinkage mechanism in which the octadecasil crystal is only peeled could not, on its own, account for the high yield of solid obtained. Thus, crystal fragmentation induced by NaOH is mainly responsible for the attainment of octadecasil nanocrystals. In support of this conclusion, a TEM image visualizing the fracture of the crystal caused by the base is included in Figure S3 in the Supporting Information.

As discussed above, treatment conditions should be carefully controlled to attain high-surface-area octadecasil with preserved crystalline structure. However, operating with an aluminum-containing zeolite is also essential. Desilication of pure SiO_2 octadecasil under the same conditions as for AT-

6 (Table 1) leads to a completely amorphous solid owing to excessive silicon dissolution (see Figure S4 in the Supporting Information). Our previous work[10b] showed that desilication of ZSM-5 in the range Si/Al = 25–50 leads to controlled mesoporosity generation. The presence of framework aluminum atoms regulates the process of silicon extraction and mesopore formation. In clathrasils, since aluminum is mostly expelled from tetrahedral framework positions during the high-temperature calcination, the leaching of silicon is likely controlled by extraframework aluminum, Al_{EF}. To support this statement, we have shown that Al_{EF} generated upon steam treatment inhibits silicon extraction and mesopore formation in ZSM-5.[10b] It is important to note that, under the desilication scheme proposed herein, there must be an aluminum gradient across the alkaline-treated crystal. The aluminum concentration in the core is considered to be essentially that of the as-made material, while the surface must be enriched. We used X-ray photoelectron spectroscopy (XPS) to measure the surface composition in the desilicated sample (Si/Al = 9), which is indeed lower than the Si/Al = 13 determined by bulk inductively coupled plasma (ICP) analysis. The XPS result, however, is not definitive, and the aluminum content at the uppermost surface could be higher, since the depth of the crystal probed by the technique (typically 5 nm) is in the order of the size of the small nanocrystals. Nevertheless, this result does support the desilication mechanism put forward. The roughness of the aluminum-rich surface could make an important contribution to the uptake in the low-pressure region of the N_2 isotherm in Figure 4 and thus to the high S_{meso} of AT-5 and AT-6.

In conclusion, this manuscript reports a novel, simple, and attractive top-down approach to prepare nanosized clathrate crystals. The result is of fundamental and applied relevance, as zeolite nanocrystals are used in a wide range of applications: catalysis, separation, adsorption, sensing, optoelectronics, medicine, and so forth.[4] The desilication treatment has been exemplified for octadecasil, although we expect it to be generally applicable to other clathrasils. The attainment of very small, stable, and aluminum-rich nanocrystals with preserved octadecasil structure and external surface areas approaching 200 $m^2 g^{-1}$ represents a step forward towards functional clathrates. For example, these nanocrystalline clathrates can be attractive supports for depositing finely dispersed metal (oxide) nanoparticles.

Finally, we questioned ourselves whether the alkaline-treated clathrasil would be active in acid-catalyzed reactions. Such reactivity is not necessarily to be expected, since strong Brønsted acidity is depleted as a consequence of the high-temperature calcination required for template removal. However, the presence of aluminum in extraframework positions is prominent (presumably $(Si/Al)_{surface} < 9$ in AT-6) and may provide Lewis acidity. As a probe reaction, calcined and alkaline-treated octadecasil were tested in catalytic pyrolysis of high-density polyethylene (HDPE). It is known that Lewis acid sites are involved in the reaction by abstraction of the hydride ion from the HDPE molecule.[15a] Besides, owing to the linear configuration of this polymer, the catalytic degradation preferentially occurs in acid sites located at the zeolite external surface,[15b] which is maximized in nanocrystals. The comparative thermogravimetric and thermal analysis profiles of selected samples are shown in Figure 5. HDPE melts at 410 K, producing exactly the same

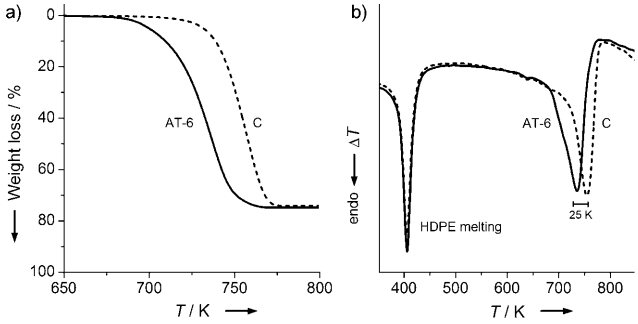

Figure 5. a) Weight loss and b) thermal analysis during pyrolysis of HDPE over calcined and alkaline-treated octadecasil samples.

endothermic transition for both samples. Calcined octadecasil is inactive, as the pyrolysis temperature of HDPE matches that of the thermal process, that is, without catalyst (not shown). In this case, the pyrolysis is initiated at 725 K. However, the pyrolysis occurs at a significantly lower temperature over the alkaline-treated sample (initiated at 675 K), thus indicating measurable catalytic action. This finding strongly points to the active nature of extraframework aluminum at the external surface. This result is relevant since, to our knowledge, no application of clathrasils in catalysis has been reported. We are aware that channel-like zeolites such as zeolite beta are considerably more active for HDPE pyrolysis.[15c] However, the main message is that clathrasils, when stabilized in the form of nanocrystals, exhibit activity and can be potentially utilized in catalysis. Thus, these results open a new window for exciting research on this type of materials.

Experimental Section

Aluminum-containing octadecasil with nominal Si/Al = 30 was synthesized hydrothermally by adapting the reported procedure[11b,12] using F^- as a mineralizer and *N,N,N*-trimethyl-*tert*-butylammonium ($TMTBA^+$) as a structure-directing agent. Briefly, aluminum nitrate was dissolved in a solution of the hydroxide form of the structure-directing agent. Then, tetraethyl orthosilicate was added to the solution and was allowed to hydrolyze. The produced ethanol and some water were evaporated at room temperature until the desired water content was achieved. The homogenized gel, with molar composition ratios Si/Al = 30, H_2O/Si = 7.1, TMTBA/Si = 0.63, and F/Si = 0.5, was transferred into a teflon-lined stainless steel autoclave and heated at 423 K for 15 days in static conditions. Finally, the solid (yield 22 wt.%) was filtered, washed, and dried overnight at 373 K. The as-synthesized octadecasil was calcined in static air at 1223 K for 5 h using a heating rate of 10 K min^{-1}. Alkaline treatments were conducted in a 16-parallel reactor system (MultiMax, Mettler Toledo) with varying temperature (318–358 K), time (15–300 min), type of base (NaOH, NH_4OH, Na_2CO_3), and base concentration (0.05–1M). The reactors (17 mm inner diameter, total volume 50 mL) were filled with alkaline solution (5 mL) and solid (166 mg) and stirred at 500 rpm. The resulting suspension was cooled in an ice bath with subsequent filtration, washing with distilled water until pH 7, and

drying at 373 K. Finally, the alkaline-treated samples were ion-exchanged in 0.1M aqueous NH_4NO_3 and calcined in static air at 723 K for 5 h. The silicon and aluminum concentrations in the solids and filtrates were determined by inductively coupled plasma optical emission spectroscopy (ICP-OES) (Perkin–Elmer Optima 3200RL (radial)). Powder X-ray diffraction (XRD) was measured using a Siemens D5000 diffractometer. Fourier transform infrared spectroscopy was carried out at 473 K in a Thermo Nicolet 5700 spectrometer using a SpectraTech Collector II diffuse reflectance (DRIFT) accessory equipped with a high-temperature chamber, ZnSe windows, and a mercury cadmium telluride (MCT) detector. Transmission electron microscopy (TEM) was carried out in a JEOL JEM-1011 microscope operated at 100 kV and equipped with a SIS Megaview III CCD camera. N_2 adsorption at 77 K was performed in a Quantachrome Autosorb-6B gas adsorption analyzer. Before the measurement, the samples were degassed in vacuum at 623 K for 12 h. X-ray photoelectron spectroscopy (XPS) measurements were obtained using a VG-Microtech Multilab 3000 spectrometer. High-density polyethylene (HDPE) pyrolysis was carried out in a Mettler Toledo TGA/SDTA851e thermobalance. The polymer and clathrasil were weighed in a 70 μL α-alumina crucible using a mass ratio polymer/zeolite = 80:20. The pyrolysis was performed in N_2 (70 mL STP min^{-1}), ramping the temperature from 373 to 973 K at 10 K min^{-1}.

Received: May 22, 2008
Published online: July 24, 2008

Keywords: clathrates · desilication · heterogeneous catalysis · nanocrystals · zeolites

[1] Ch. Baerlocher, W. M. Meier, D. H. Olson, *Atlas of Zeolite Framework Types*, *5th ed.*, Elsevier, Amsterdam, **2001**.

[2] a) S. Ernst, *Angew. Chem.* **1996**, *108*, 67; *Angew. Chem. Int. Ed. Engl.* **1996**, *35*, 63; b) A. Corma, *Chem. Rev.* **1997**, *97*, 2373; c) M. Hartmann, *Angew. Chem.* **2004**, *116*, 6004; *Angew. Chem. Int. Ed.* **2004**, *43*, 5880; d) A. Taguchi, F. Schüth, *Microporous Mesoporous Mater.* **2005**, *77*, 1; e) J. C. Groen, W. Zhu, S. Brouwer, S. J. Huynink, F. Kapteijn, J. A. Moulijn, J. Pérez-Ramírez, *J. Am. Chem. Soc.* **2007**, *129*, 355.

[3] A. Corma, M. J. Díaz-Cabañas, J. L. Jordá, C. Martínez, M. Moliner, *Nature* **2006**, *443*, 842.

[4] a) L. Tosheva, V. P. Valtchev, *Chem. Mater.* **2005**, *17*, 2494; b) S. C. Larsen, *J. Phys. Chem. C* **2007**, *111*, 18464.

[5] A. Corma, U. Diaz, M. E. Domine, V. Fornés, *Angew. Chem.* **2000**, *112*, 1559; *Angew. Chem. Int. Ed.* **2000**, *39*, 1499.

[6] a) D. Trong-On, S. Kaliaguine, *Angew. Chem.* **2001**, *113*, 3348; *Angew. Chem. Int. Ed.* **2001**, *40*, 3248; b) J. Čejka, S. Mintova, *Catal. Rev. Sci. Eng.* **2007**, *49*, 457.

[7] a) S. van Donk, A. H. Janssen, J. H. Bitter, K. P. de Jong, *Catal. Rev. Sci. Eng.* **2003**, *45*, 297; b) C. H. Christensen, K. Johannsen, I. Schmidt, C. H. Christensen, *J. Am. Chem. Soc.* **2003**, *125*, 13370; c) Y. Tao, H. Kanoh, L. Abrams, K. Kaneko, *Chem. Rev.* **2006**, *106*, 896; d) M. Choi, H. S. Cho, R. Srivastava, C. Venkatesan, D.-H. Choi, R. Ryoo, *Nat. Mater.* **2006**, *5*, 718; e) J. C. Groen, J. A. Moulijn, J. Pérez-Ramírez, *J. Mater. Chem.* **2006**, *16*, 2121.

[8] a) K. Egeblad, C. H. Christensen, M. Kustova, C. H. Christensen, *Chem. Mater.* **2008**, *20*, 946, and references therein; b) J. Pérez-Ramírez, C. H. Christensen, K. Egeblad, C. H. Christensen, J. C. Groen, *Chem. Soc. Rev.* **2008**, DOI: 10.1039/b809030k.

[9] H. Gies, B. Marler, U. Werthmann in *Molecular Sieves: Science and Technology*, *Vol. 1* (Eds.: H. G. Karge, J. Weitkamp), Springer, Heidelberg, **1998**, pp. 35 – 64.

[10] a) M. Ogura, S.-Y. Shinomiya, J. Tateno, Y. Nara, M. Nomura, E. Kikuchi, M. Matsukata, *Appl. Catal. A* **2001**, *219*, 33; b) J. C. Groen, L. A. A. Peffer, J. A. Moulijn, J. Pérez-Ramírez, *Chem. Eur. J.* **2005**, *11*, 4983; c) X. Wei, P. G. Smirniotis, *Microporous Mesoporous Mater.* **2006**, *97*, 97; d) J. C. Groen, T. Sano, J. A. Moulijn, J. Pérez-Ramírez, *J. Catal.* **2007**, *251*, 21.

[11] a) P. Caullet, J. L. Guth, J. Hazm, J. M. Lamblin, H. Gies, *Eur. J. Solid State Inorg. Chem.* **1991**, *28*, 345; b) L. A. Villaescusa, P. A. Barrett, M. A. Camblor, *Chem. Mater.* **1998**, *1012*, 3966; c) L. A. Villaescusa, Ph. D. thesis, Universidad Politécnica de Valencia, **1999**.

[12] L. A. Villaescusa, F. M. Márquez, C. M. Zicovich-Wilson, M. A. Camblor, *J. Phys. Chem. B* **2002**, *106*, 2796.

[13] A. Zecchina, S. Bordita, G. Spoto, L. Marchese, G. Petrini, G. Leofanti, M. Padovan, *J. Chem. Soc. Faraday Trans.* **1992**, 2959.

[14] B. C. Lippens, J. H. de Boer, *J. Catal.* **1965**, *4*, 319.

[15] a) D. W. Park, J. R. Kim, J. K. Choi, Y. A. Kim, H. C. Woo, *Polym. Degrad. Stab.* **1999**, *65*, 193; b) D. P. Serrano, J. Aguado, J. M. Escola, J. M. Rodríguez, *J. Anal. Appl. Pyrolysis* **2005**, *74*, 353; c) J. Agulló, N. Kumar, D. Berenguer, D. Kubicka, A. Marcilla, A. Gómez, T. Salmi, D. Yu. Murzin, *Kinet. Catal.* **2007**, *48*, 535.

